Kara J. Levinson, PhD, MPH[4]; Linda S. Thomas, MPH, MAFM, BSMT (ASCP)[4]; Zachary Perry, BS[4]; Krista Queen, PhD[5]; Anna Uehara, PhD, MScGH[6]; Suxiang Tong, PhD[5]; Ying Tao, PhD[6]; Mary-Margaret A. Fill, MD[7]; Timothy F. Jones, MD[7]; William Schaffner, MD[8]; John R. Dunn, DVM, PhD[7]; [1]Centers for Disease Control and Prevention, Nashville, TN; [2]Knox County Health Department, Knoxville, Tennessee; [3]University of Tennessee, Knoxville, Tennessee; [4]Division of Laboratory Services, TN Department of Health, Nashville, Tennessee; [5]Division of Viral Diseases, Centers for Disease Control and Prevention (CDC), Atlanta, Georgia; [6]Centers for Disease Control and Prevention (CDC), Atlanta, Georgia; [7]Tennessee Department of Health, Nashville, Tennessee; [8]Vanderbilt University Medical Center, Nashville, Tennessee

Session: O-37. Updates in COVID Epidemiology

Background. Human-to-feline and airborne transmission among cats of Severe Acute Respiratory Syndrome Coronavirus-2 (SARS-CoV-2) has been described, though documented feline-to-human transmission has not been reported. In October 2020, all 3 Malayan tigers at a Tennessee AZA accredited zoo were diagnosed with symptomatic SARS-CoV-2 infection. We investigated to determine source and prevent further transmission.

Methods. Tiger nasal swab specimens were tested at the National Veterinary Services Laboratories (NVSL). An environmental assessment at the zoo was completed. We interviewed 18 staff who interacted with the tigers during the 2 weeks before animal symptom onset. Confirmed human cases were defined as persons testing positive for SARS-CoV-2 by RT-PCR during September 28–October 29, with tiger interaction during their 14-day incubation period. Interviewed staff had repeat SARS-CoV-2 RT-PCR and serum IgG testing on October 29. Tigers and staff testing positive had specimens sent to CDC for genomic sequencing. Tiger sequences were compared phylogenetically with 30 geographically associated human cases collected within 2 weeks of the outbreak and > 200 background sequences from TN.

Results. NVSL confirmed SARS-CoV-2 infection in all 3 tigers. Environmental assessment identified fencing between humans and animals allowing airflow and an open outdoor exhibit observation point above the habitat. Confirmed cases were identified in a tiger keeper and veterinary assistant; both developed symptoms after exposure to symptomatic tigers and one sample was genotyped. Staff did not report known contact with ill visitors. All staff were negative for SARS-CoV-2 IgG. The tigers and most temporally and geographically associated cases had genetic sequences in clade 20G and B.1.2. Tiger sequences were 3-6 single nucleotide polymorphisms different from the positive tiger keeper (Figure).

Figure. Whole-genome phylogenetic analysis.

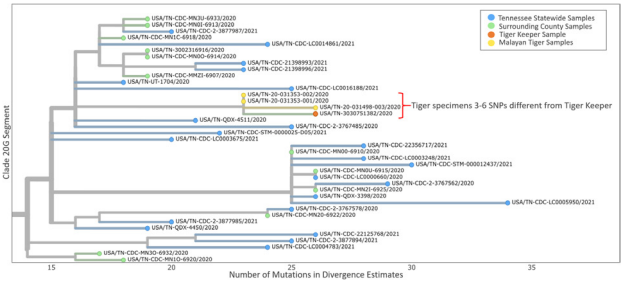

Whole-genome phylogenetic analysis from a portion of clade 20G showing divergence estimates from SARS-CoV-2 Wuhan-Hu-1 reference genome with sequences from humans living in Tennessee and Malayan tigers sampled during the outbreak investigation in October 2020. Sequence analysis showed 3-6 single nucleotide polymorphisms (SNPs) differences between one human tiger keeper and all three tiger sequences. Differences are indicated by one-step edges (lines) between colored dots (individual SARS-CoV-2 sequenced infections). Numbers indicate unique sequences. Note not all analyzed sequences are shown in this figure.

Conclusion. Using a One Health approach, we concluded the index tiger was likely infected via transmission from an ill visitor at an exhibit observation point or unidentified asymptomatic staff. Infection spread to the other 2 tigers and tiger-to-human transmission to 2 staff is possible thereafter. The zoo was advised on infection control practices for humans and animals, and no additional cases were identified.

Disclosures. **William Schaffner, MD**, **VBI Vaccines** (Consultant)

190. Epidemiology of COVID-19 Breakthrough Infections in Dallas County, Texas, 2021

Suzanne Wada, MD[1]; Jared Wiegand, MPH[1]; Mary Markarian, RN[1]; Victoria Hung, BS[1]; Christina Zhu, BS[1]; Megin Parayil, MPH[1]; Kyoo Shim, MPH[2]; Jose Serrano, MPH[1]; Wendy Chung, MD, MS[1]; [1]Dallas County Health and Human Services, Dallas, Texas; [2]Dallas County Department of Health and Human Services, Dallas, TX

Session: O-37. Updates in COVID Epidemiology

Background. From March 2020 through May 2021, Dallas County reported a total of 304,056 cases of COVID-19, including 4,073 deaths. During the month of December 2020, a post-holiday surge of cases led to peak daily average case rates of over 50 cases per 100,000. COVID-19 cases and deaths have since declined substantially following the rollout of COVID-19 vaccine delivery. As of June 8, 2021, about 1,831,588 Dallas County residents have received at least one COVID-19 vaccine dose and 910,067 are fully vaccinated. Recent county integration of immunization and case databases enabled identification and analysis of COVID-19 breakthrough infections.

Methods. A COVID-19 breakthrough infection was defined as a positive test (PCR or antigen) collected from an individual ≥ 14 days after receiving the full series of an FDA-authorized COVID-19 vaccine. Nationally, 10,262 vaccine breakthrough infections had been reported from 46 US states and territories, through April 2021. Vaccine breakthrough cases were reviewed and medical records abstracted to collect demographic information, clinical characteristics, and medical conditions. Data analysis was performed using R, version 4.0.2 (2020).

Results. Of the 700 vaccine breakthrough cases reported in Dallas County residents as of June 8, 2021, 304 (43%) were male and 396 (57%) female, with an average age of 53 years. The majority of the vaccine breakthrough cases were White (42%); 25% were Hispanic/Latino; and 20% were Black. Almost all breakthrough cases were confirmed with PCR testing, with 451 (64%) cases receiving the Pfizer vaccine. Of breakthrough cases, 49% were symptomatic; 52% (358) had underlying conditions including: tobacco use, obesity, or immunocompromised state; 68 (10%) were hospitalized; and 11 (1.6%) died. Whole genome sequencing was performed on 51 cases, with 14 (27.5%) variants identified, including: eight B.1.1.7, two B.1.429 and one P.1 variants.

Conclusion. Despite the high levels of vaccine efficacy documented in US vaccine trials, COVID-19 breakthrough infections, though currently uncommon, do occur and are important to investigate. Ongoing close public health surveillance of variants is needed to discern changes in patterns of vaccine efficacy and characteristics of populations at greatest risk of severe disease from COVID-19.

Disclosures. **All Authors**: No reported disclosures

191. High-Dose Rifampin-containing Regimens for the Treatment of TB Meningitis

Camilo A Ruiz-Bedoya, MD[1]; Filipa Mota, PhD[2]; Elizabeth Tucker, MD[2]; Farina Mahmud, PhD[2]; Clara Erice, PhD[1]; Melissa Bahr, BS[1]; Kelly Flavahan, n/a[2]; Patricia De Jesus, Bs[1]; John Kim, Bs[1]; Marina Da Costa Rosa, Msc[1]; Alex Shimura Yamashita, PhD[1]; Catherine A Foss, PhD[1]; Charles A. Peloquin, Pharm.D.[3]; Charles A. Peloquin, Pharm.D.[3]; Alvaro A. Ordonez, MD[2]; Sanjay K. Jain, MD[2]; Sanjay K. Jain, MD[2]; [1]Johns Hopkins University, School of Medicine, Baltimore, MD; [2]Johns Hopkins, Baltimore, Maryland; [3]University of Florida, Gainesville, FL

Session: O-38. Updates in Mycobacteria

Background. TB meningitis is the most severe form of tuberculosis (TB), associated with high morbidity and mortality. High-dose rifampin (35mg/kg/day) is safe in adults and substantially improves the bactericidal activity of standard TB regimen. However, there is conflicting data regarding its benefit in TB meningitis where outcomes may also be associated with intracerebral inflammatory responses.

Methods. A novel mouse and a validated rabbit model of TB meningitis utilizing intracranial *Mycobacterium tuberculosis* infections were used for these studies (**Fig. 1**). Animals received high-dose (35 mg/kg/day) or standard-dose (10 mg/kg/day) rifampin in combination with isoniazid, pyrazinamide and dexamethasone at human equipotent dosing. Bacterial burden, multi-modality positron emission tomography (PET) imaging, tissue drug concentrations, markers of neuroinflammation, and vascular leak were measured. Imaging data from a patient with TB meningitis was analyzed and correlated with the findings in animals.

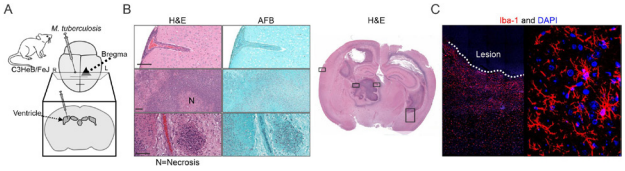

Figure 1. Mouse model of TB meningitis replicates human histopathology hallmarks. (A) Scheme of infection. (B) Histopathology hematoxylin-eosin (H&E) and acid-fast bacilli (AFB) staining in a representative M. tuberculosis-infected mouse shows regions of meningitis, ventriculitis, choroiditis, necrotizing and non-necrotizing granulomas. The bar represents 100μm. (C) Images show immunofluorescence of microglia activation in red (Iba-1) and nuclear stain in blue (DAPI). The rabbit model of TB meningitis has been described previously (Tucker et al. Dis Model Mech. 2016 and Tucker et al. Sci Transl Med. 2018). Animal studies were approved by the Johns Hopkins Animal Care and Use Committee.

Results. Administration of the high-dose rifampin regimen achieved four times higher brain concentration than the standard-dose regimen and displayed higher bactericidal activity in both mice and rabbits ($P < 0.01$) (**Fig. 2**). There were no differences in intracerebral microglial activation (^{124}I-DPA-713 PET and iDISCO) and pro-inflammatory cytokines during treatment in animals receiving high- or standard-dose rifampin regimens (**Fig. 3**). Whole-brain PET and immunolabeling demonstrated spatially compartmentalized inflammation, vascular leak and rifampin exposures (**Fig. 4**). Longitudinal imaging in the same animals showed a 40% decrease in vascular leak after two weeks of TB treatment. Spatially compartmentalized brain rifampin exposures and decreases in vascular edema over TB treatment were also noted in the TB meningitis patient.

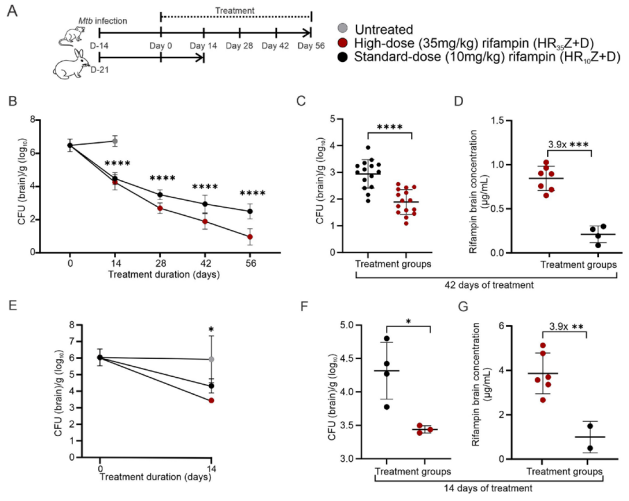

Figure 2. High-dose rifampin treatment in mouse and rabbit models of TB meningitis. (A) Experimental scheme. R10 (rifampin 10mg/kg), R35 (rifampin 35mg/kg), H (isoniazid), Z (pyrazinamide), D (dexamethasone). (B) Bactericidal activity of high-dose rifampin (n = 60 animals) and standard-dose rifampin (n = 60 animals) regimens in mice. (C) Grouped colony forming units (CFU) and (D) rifampin brain concentration in mice after 42 days of TB treatments. (E) Bactericidal activity of high-dose rifampin (n = 4 animals) and standard-dose rifampin (n = 3 animals) regimens in rabbits. Data from untreated rabbits (n = 2 animals) is also shown. (F) Grouped CFU and (G) rifampin brain concentration in rabbits after 14 days of TB treatments. Tissues were assayed using validated ultra-high-performance liquid chromatography and tandem mass spectrometry (LC-MS/MS) for rifampin at the Infectious Diseases Pharmacokinetics Laboratory of the University of Florida. The bacterial burden is represented as CFU per gram of tissue and presented on a logarithmic scale. CFU and mass spectrometry data are represented as mean ± SD. *P < 0.05, **P < 0.01 and ***P < 0.001 calculated using a two-way ANOVA test.

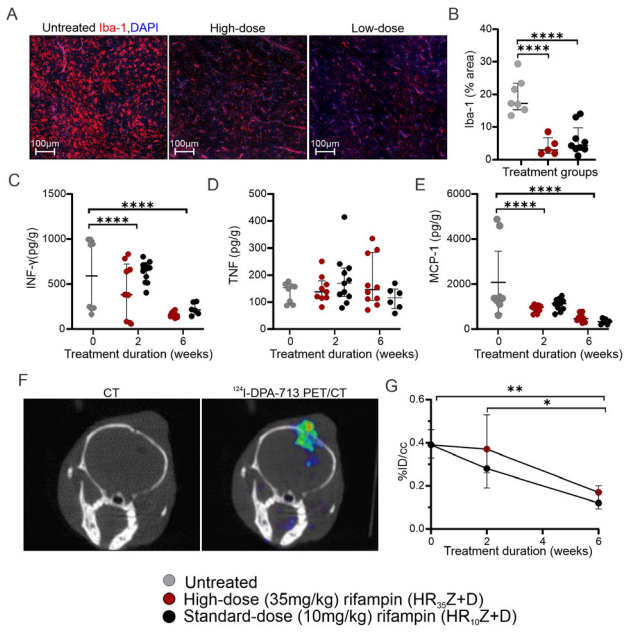

Figure 3. Neuroinflammatory responses during TB treatment. (A) Iba-1 and DAPI immunofluorescence in a representative untreated, high-dose and low-dose-treated mouse. (B) Quantification of Iba-1 immunofluorescence before treatment and after 6 weeks of treatment (n = 3 mice per group). Sections were imaged at 40X with Nikon A1+ confocal microscope. HALO was used for visualization and quantification. Quantification of intraparenchymal (C) INF-γ, (D) TNF and (E) MCP-1 in untreated and treated mice (Milliplex Multiplex Luminex assay). (F) Coronal CT and 124I-DPA-713 PET/CT of a representative mouse with TB meningitis before treatment initiation. (G) 124I-DPA-713 PET quantification before treatment (n = 15 animals) and after 2 (n = 5 animals per group) and 6 (n = 5 animals per group) weeks of TB treatment. PET data is represented as median ± IQ. *P < 0.05, **P < 0.01 and ***P < 0.001 were calculated using a two-way ANOVA test.

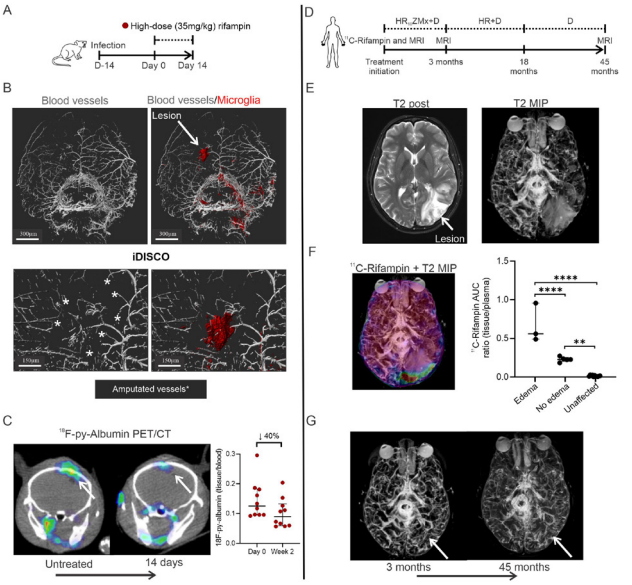

Figure 4. Changes in vascular leakage and rifampin penetration during TB treatment. (A) Experimental scheme in mice. (B) Whole-brain immunolabeling (iDISCO) of a representative M. tuberculosis-infected mouse prior to treatment initiation. Images show immunolabeling of α-smooth muscle actin in grey and microglia activation in red (Iba-1). Asterix represents the areas of vascular amputation. (C) Coronal 18F-py-Albumin PET/CT and quantification (tissue to plasma ratio) in untreated and 2 weeks-treated mice (n = 10 animals at each time-point). (D) Serial imaging in a patient with TB meningitis. (E) Transverse T2 post-contrast section and maximal intensity projection (MIP) showing vasogenic edema. (F) Co-registered T2 post-contrast MIP with transverse 11C-rifampin area under the curve (AUC) heat-map, and 11C-rifampin tissue to plasma ratio quantification of the areas with and without vasogenic edema, and unaffected brain. (G) T2 post-contrast MIP at 3 and 45 months after treatment initiation. The patient with TB meningitis was recruited as part of a 11C-rifampin PET research study performed under the U.S. FDA Radioactive Drug Research Committee program for investigational drugs (Tucker et al. Sci Transl Med. 2018; Ordonez et al. Nat Med. 2020). Human studies were approved by the Johns Hopkins University Institutional Review Board Committee. M = moxifloxacin. PET data is represented as median ± IQ. *P < 0.05, **P < 0.01 and ***P < 0.001 calculated using a two-way ANOVA test.

Conclusion. Our cross-species findings suggest that an intensified high-dose rifampin regimen is more efficacious than the standard treatment for TB meningitis without an increase in neuroinflammation. Vascular leak decreases during TB treatment and may account for decreases in rifampin permeability over time. These studies have important implications for antimicrobial development for TB meningitis.

Disclosures. **Charles A. Peloquin, Pharm.D.**, Nothing to disclose **Alvaro A. Ordonez, MD**, **Cubresa** (Consultant)**Fujirebio Diagnostics** (Research Grant or Support) **Sanjay K. Jain, MD**, **Fujirebio Diagnostics, Inc., USA** (Research Grant or Support)**Novobiotic LLC, USA** (Research Grant or Support)**T3 Pharma, Switzerland** (Research Grant or Support) **Sanjay K. Jain, MD**, Fujirebio Diagnostics, Inc., USA (Individual(s) Involved: Self): Research Grant or Support; Novobiotic LLC, USA (Individual(s) Involved: Self): Research Grant or Support; T3 Pharma, Switzerland (Individual(s) Involved: Self): Research Grant or Support

192. Tolerability Outcomes of Multi-drug Antibiotic Treatment for Pulmonary Nontuberculous Mycobacterial Disease due to *Mycobacterium avium* Complex in U.S. Medicare Beneficiaries with Bronchiectasis

Jennifer Ku, MPH[1]; Emily Henkle, PhD, MPH[1]; Kathleen F. Carlson, PhD MS[1]; Miguel Marino, PhD[1]; Sarah K. Brode, MD[2]; Theodore K. Marras, MD[2]; Kevin L. Winthrop, MD, MPH[1]; Kevin L. Winthrop, MD, MPH[1]; [1]Oregon Health & Science University, Portland, OR; [2]University Health Network and University of Toronto, Toronto, Ontario, Canada

Session: O-38. Updates in Mycobacteria

Background. Nontuberculous mycobacteria (NTM), most frequently *Mycobacterium avium* complex (MAC), cause increasingly common pulmonary infections. Treatment interruptions and early discontinuation are common in MAC therapy, but population-based data on treatment outcomes are severely lacking. We examined tolerability outcomes of guideline-based 3-drug therapies (GBT) targeted for pulmonary MAC infection.

Methods. Among beneficiaries with bronchiectasis (ICD-9-CM 494.0 or 494.1) in U.S. Medicare data (01/2006 – 12/2014), we identified first-time MAC GBT therapy users, excluding those with cystic fibrosis, HIV, or a history of organ transplant. MAC GBT was defined as an overlapping prescription of ≥ 28-day supply of a macrolide, ethambutol and rifamycin. Using Cox regression methods, we compared time-to-regimen